The Impact of Huge Structural Changes on Electron Transfer and Measurement of Redox Potentials: Reduction of ortho-12-Carborane

John R. Miller[1], Andrew R. Cook[1], Ludmila Šimková [2], Lubomír Pospíšil [2], Jiří Ludvík[2] and Josef Michl[3,4]*

[1] Chemistry Division, Brookhaven National Laboratory, Upton, NY 11973 USA.

[2] J. Heyrovský Institute of Physical Chemistry of the Czech Academy of Sciences, Dolejškova 3, Prague 8, CZ-18223, Czech Republic

[3] Department of Chemistry, University of Colorado, Boulder, Colorado 80309-0215 USA.

[4] Institute of Organic Chemistry and Biochemistry, Czech Academy of Sciences, Flemingovo nam. 2, Prague 6, CZ-16610, Czech Republic.

KEYWORDS: Homogeneous vs.heterogeneous electron transfer, reorganization energy, cyclic voltammetry, pulse radiolysis, overpotential, Frumkin Effect, free energy relation, carborane

ABSTRACT

A massive structural change accompanies electron capture by the 1,2-dicarba-*closo*-dodecaborane cage molecule (**1**). Bimolecular electron transfer (ET) by pulse radiolysis found a

reduction potential of E^0= -1.92 V vs. $Fc^{+/0}$ for **1** and rate constants that slowed greatly for ET to or from **1** when the redox partner had a potential near this E^0. Similarly, two electrochemical techniques could detect no current at potentials near E^0, finding instead peaks or polarographic waves near -3.1 V, which is 1.2 V more negative than E^0. Voltammetry could determine rate constants, but only near -3.1 V. DigiSim simulations require electrochemical rate constants near $1x10^{-10}$ cm/s at E^0, a factor of 10^{-10} relative to molecules undergoing facile ET. This factor of 10^{-10} compared to ~10^{-5} for bimolecular ET presents a puzzle. We propose that a manifestation of one of the "Frumkin Effects" in which only part of the applied voltage is available to drive ET at the electrode provides a resolution to this puzzle.

Introduction

The Marcus Theory identifies reorganization energies, which arise from changes in the structure of molecules and surrounding solvent during electron transfer (ET), as principal factors controlling electron transfer rates.[1,2] For efficient use in energy storage, including photosynthesis, ET reactions should be accompanied by small reorganization energies.[3] Still investigation of ET with large reorganization energy can provide valuable windows into how ET works. Figure 1 pictures the computed structure of 1,2-dicarba-*closo*-dodecaborane cage molecule (**1**) in three oxidation states.

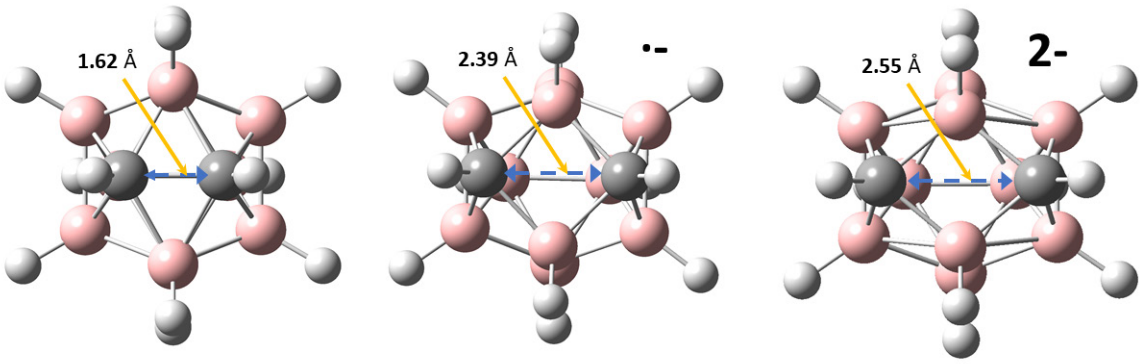

Figure 1. Optimized structures (b3lyp/6-31g(d)) of **1**. The neutral (left) is a nearly dodecahedryl *closo*-carborane having a C-C bond length of 1.62 Å. In the radical anion the C-C bond length expands to 2.39 Å and further in the dianion to 2.55 Å to become a *nido* structure (right).

The massive structural change pictured in Figure 1 will be seen to have astonishing effects on electrochemistry, energetics and rates of ET of **1**. They are consistent with earlier results by Zhang and Bowen.[4] Experiments have shown that [5-10] large structural changes produce changes in rate constants for electrochemical ET,[5-7] homogeneous self-exchange ET,[8,9,10 ,11,12] heterogeneous bimolecular ET and can markedly alter the appearance of voltammetric waves.[5,6] For crowded ethylene derivatives Evans and coworkers[5-7] found distinct isomers that were roughly planar and perpendicular, with measurable reduction potentials for each. Their chemistry and electrochemistry was usually best described with separate steps in a "square" scheme. Here we seek to understand the effects of the different structure change of **1** and learn whether it follows similar or different mechanism.

Experimental

Electrochemical measurements were performed using an analog potentiostat PA4 (Laboratorní přístroje Praha) and/or a digital computer-controlled instrument PGSTAT 101 (AUTOLAB, Switzerland). AC polarography used a fast rise-time potentiostat, a lock-in amplifier (Stanford Research, model SRS830), and a frequency response analyzer (Stanford Research, model SRS760). Cyclic voltammetry (CV) utilized platinum, glassy carbon, hanging mercury drop electrode (HMDE), gold and boron-doped diamond (BDDE**)** electrodes with saturated calomel electrode (SCE) as a reference electrode. The potential of ferrocene (Fc) oxidation was 0.545 vs. SCE. DC polarography with dropping mercury electrode (DME) used a capillary with ∅ =47μm and controlled drop times of 1s. The combination of methods yielded a large working range from 1.7 to –2.95 V vs. SCE.

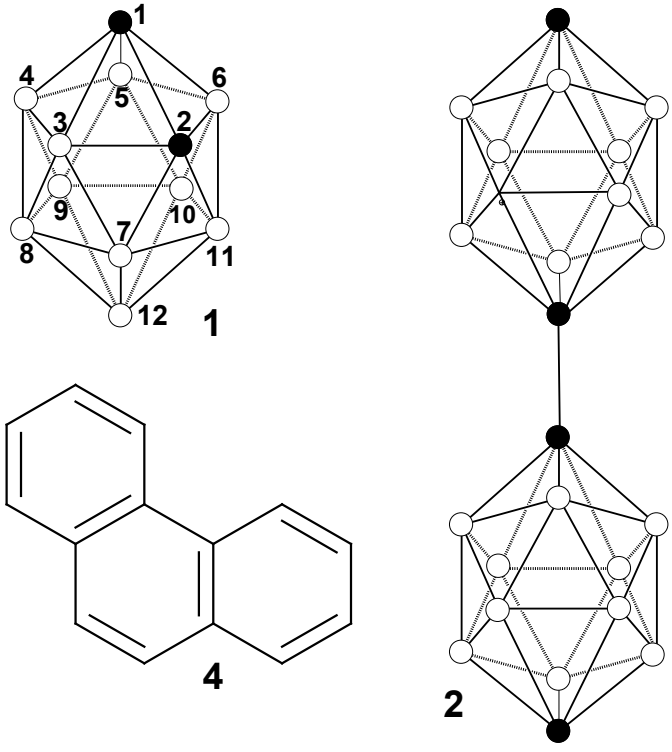

Chart 1. Structures of compounds used in this study. For **1** the vertices are numbered, showing carbons ● and borons ○. Compound **3** (not shown), 1,2-dicarba-4,5,7,8,9,10,11,12-octamethyl-*closo*-dodecaborane[13] , is similar to **1** but bears methyl groups on eight of the boron atoms.

Pulse radiolysis was carried out using the Laser Electron Accelerator Facility with an electron pulse of < 50 ps duration at Brookhaven National Laboratory; methods of measurement are described elsewhere.[14] Briefly, the 9 MeV electrons created solvent ionization in samples in high purity silica cells with optical path lengths of 2 cm containing the molecules under study in purified THF under argon. Solvated electrons from ionization events were then captured by solute molecules, and rates determined. The monitoring light source was a pulsed Xenon arc lamp. The probing wavelength was selected by 10 nm bandpass optical interference filters. Transient absorption signals were detected by a silicon photodiode (EG&G FND-100Q, 2 ns response time) and digitized by LeCroy 8620A or 640Zi oscilloscope.

Computations used Gaussian 16[15] and electrochemical simulations used DigiSim.[16]

Results

Voltammetry of 1. Determination of energies associated with electron addition or removal often utilize electrochemical approaches. The most reliable is a combination of a steady-state method (DC-polarography or rotating disk voltammetry) with a dynamic one (cyclic voltammetry - CV) using various electrode materials. No electrochemical oxidation of **1** was observed in the entire range in agreement with computations (Table 1) but Figure 2a shows CVs for electrochemical reduction of **1 (**for the corresponding polarographic curve see Figure S2). While reversible or partly-reversible CV's have been reported for other molecules undergoing large structural changes[17] the thermodynamically relevant reduction potential of **1** could not be clearly determined because the CV in Figure 2, which shows a cathodic peak at –3.1 V vs. $Fc^{+/0}$, is totally irreversible showing no return anodic counterpeak. Current in the reduction corresponds

to 1.7± 0.2 electrons per **1** molecule. Below we employ additional electrochemical methods and pulse radiolysis seeking to determine the reversible potential, electron transfer rate constants and the mechanism of reduction.

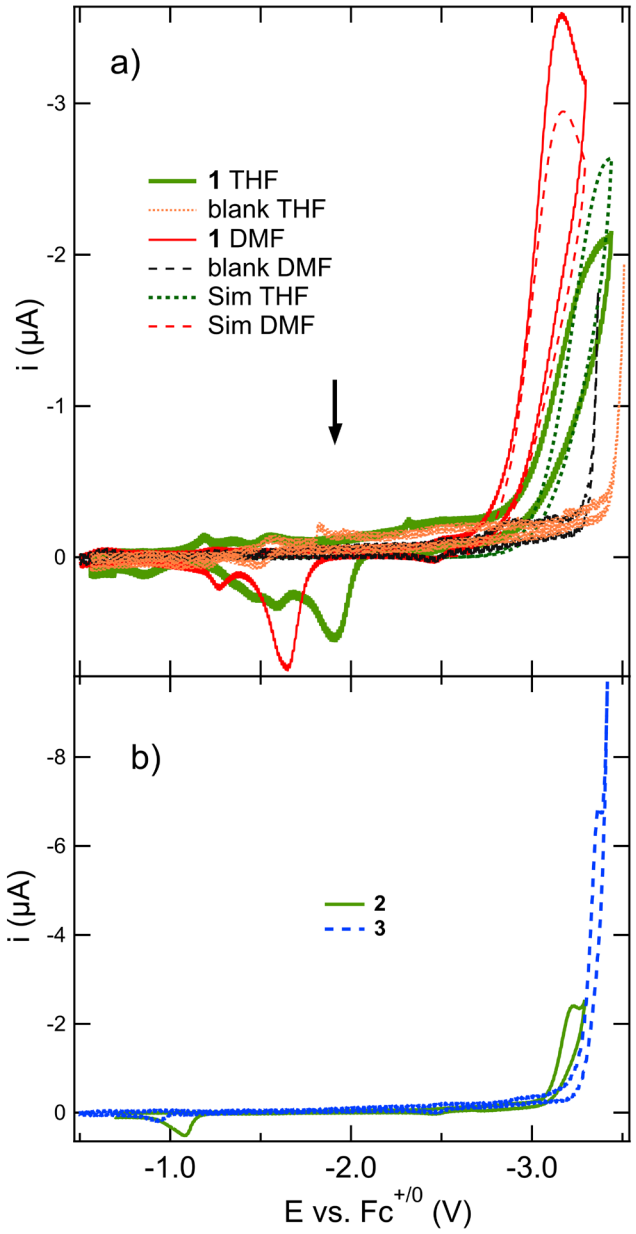

Figure 2. a) Cyclic voltammogram (first scan) of ~1 mM of **1** at the HMDE in THF and DMF, 100 mV/s. A simulation is shown assuming a 0.375 mm drop, $E^0 = -1.92$ and $k_s = 2\times10^{-10}$ cm/s and a 2nd reduction at $E^0 = -1.82$ V with k_s=0.01 cm/s followed by protonation with $K_{eq} = 1\times10^3$ and $k = 1\times10^8$ $M^{-1}s^{-1}$. A vertical arrow marks E^0(**1**) determined below. b) Cyclic voltammetry of **2** and **3** in DMF with 0.1 M $TBAPF_6$ on HMDE.

The simulations in Figure 2a use the Marcus-Hush (MH) form in Digisim[16] with $k^0 = 2\times10^{-10}$ cm/s^{-1} and a reorganization energy of 2.16 eV, based on findings below (see Figure 3), which also identify the reversible redox potential as -1.92 V vs. $Fc^{+/0}$. It is essential here not to use the Butler-Volmer equation.[18] With the large voltage difference between E^0 and the CV peak the Marcus-Hush form is much more accurate.[19] The simulations were informed by computed results in Table 1. The second reduction to form the dianion $\mathbf{1}^{-2}$ is consistent with observations that **1** was reduced to $\mathbf{1}^{-2}$ by NaK[20] or BuLi[21] and that $\mathbf{1}^{-2}$ transferred an electron to benzophenone (E^0=-2.21 [22]) to form benzophenone$^{\bullet-}$.[20] This latter observation is consistent with the rough estimate $E^0 = -1.82$ V for the 2nd reduction used in the simulation.

Cyclic voltammograms similar to those in Figure 2 were recorded in DMF and THF at HMDE and at glassy carbon electrodes, all of which show peaks/polarographic waves near –3.1 V vs. $Fc^{+/0}$ (Figures S1-S3) confirming that neither solvent, nor electrode material influence substantially the apparent electrochemical reduction potential.

Bimolecular ET Rate Constants When **1** was placed in THF solution along with a variety π-molecules having known, reversible potentials, it was possible to observe electron transfer

reactions from radical anions of the π-molecules to **1** or from **1** radical anions to π-molecules having more positive redox potentials:

$$D^{\bullet-} + \mathbf{1} \rightarrow D + \mathbf{1}^{\bullet-} \qquad (1)$$

$$\mathbf{1}^{\bullet-} + A \rightarrow D + A^{\bullet-} \qquad (2)$$

The radical anions were produced by capture of solvated electrons in pulse radiolysis experiments. While $\mathbf{1}^{\bullet-}$ was difficult to observe because it absorbs only weakly in the UV range, reactions (1) and (2) were readily followed by transient absorption of $D^{\bullet-}$ or $A^{\bullet-}$. Examples are shown in Figures S4-S7. Rate constants determined for these bimolecular electron transfer reactions to **1** (reaction 1) or from $\mathbf{1}^{\bullet-}$ (reaction 2) are plotted in Figure 3 against the known redox potentials of the molecules D and A. In Figure 3 we see that the radical anion of any molecule, D, transfers an electron to **1** if the redox potential, $E^0(D^{0/-})$ is more negative than –1.9 V vs. $Fc^{+/0}$. Conversely any molecule, A, having a redox potential $E^0(A^{0/-})$ more positive than –1.9 V vs. $Fc^{+/0}$ can accept an electron from $\mathbf{1}^{\bullet-}$ to produce $A^{\bullet-}$. Solid curves in Figure 3 are fits to the two sets of data, $D^{\bullet-}$ + **1** and $\mathbf{1}^{\bullet-}$ + A, using ET theory as described in the discussion.

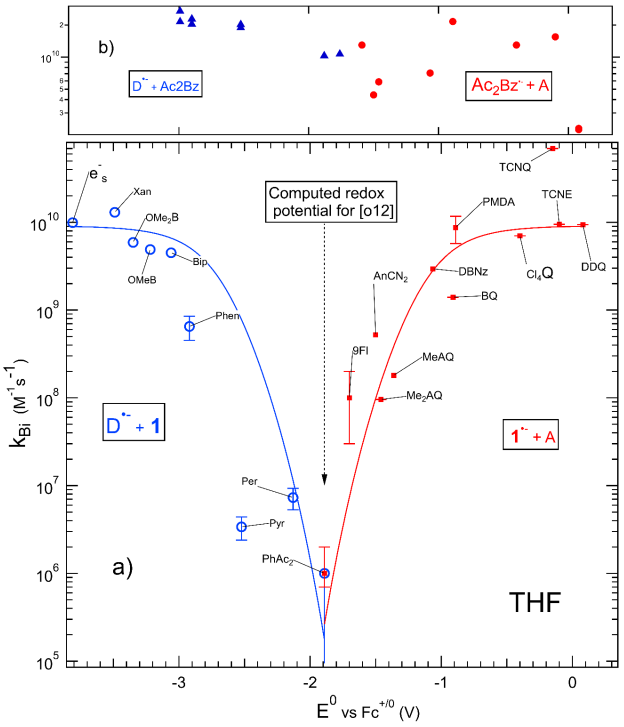

Figure 3. a) Rate constants for ET from radical anions, $D^{\bullet-}$ to **1** (o) and from $\mathbf{1}^{\bullet-}$ to a series of acceptors, A, (■) in THF plotted as functions of redox potentials of the donors, D, and acceptors, A. b) A similar graph for ET to and from 1,4-diacetylbenzene, which will be seen below to have a reduction potential almost identical to that of **1**.

The fit curves shown in Figure 3 describe the rates in terms of electron transfer theory limited by diffusion-control. The lines in Figure 3 are fits to the familiar expression for nonadiabatic electron transfer[2,23-26] with solvent and internal reorganization energies. Internal reorganization is represented by a single vibrational mode.

$$k_{ET} = \frac{2\pi}{\hbar}|H_{ab}(r)|^2 \,\mathrm{FCWD} \qquad (3)$$

$$\mathrm{FCWD} = (4\pi\lambda_s k_B T)^{-1/2} \sum_{w=0}^{\infty}\left(e^{-S}\frac{S^w}{w!}\right)\exp\{-[(\lambda_s + \Delta G^o + w\hbar\omega)^2 / 4\lambda_s k_B T]\}$$

$S = \lambda_v/\hbar\omega$.

$$k_{Bi}^{-1} = k_{act}^{-1} + k_d^{-1} \qquad (4)$$

Integration[25,26] over all space with

$$|H_{ab}(r)|^2 = |H_{ab}(R_0)|^2 \exp(-\beta r) \qquad (5)$$

of the distant-dependent ET rate gives the electron transfer rate without diffusion, k_{act}, which is close to the rate constant at contact distance, R_0. Waite's expression[27] (4) gives the overall bimolecular rate constant including diffusion-control, k_{Bi}, which is plotted in the fit curves compared with the data in Figure 3.

The electron transfer reactions for which rate constants were plotted in Figure 3a) all went to completion with the exception of the reaction with 1,4-diacetylbenzene (Ac_2Bz). This electron transfer reaction was sufficiently slow that substantial (~50%) of $Ac_2Bz^{\bullet-}$ decayed during the time equilibrium was established. While the extensive decay created ambiguity, it was possible to conclude that electron transfer from $Ac_2Bz^{\bullet-}$ to **1** went to an equilibrium with K_{eq} = 0.29 ± 0.08, ΔG^o = 32 ± 10 meV. This with Pedersen's reduction potential $E^0(Ac_2Bz)$= –1.887 V vs. $Fc^{+/0}$ [22] yields $E^0(\mathbf{1}^{0/-})$ = –1.92 ± 0.01 V vs. $Fc^{+/0}$. In separate experiments, rate constants to and from Ac_2Bz with the same D and A used with **1** show little variation with redox potential (Figure 3b); all lie near the diffusion-controlled limit.

Fits for ET rates vs. redox potentials corroborate this -1.92 V potential, which is more than 1 V positive of the –3.1 V position of the irreversible wave seen in Figure 2. Verification of this astonishing > 1 V difference was sought using electrochemical catalysis, AC Voltammetry, impedance spectroscopy, and ab initio computations described below.

Electrochemical Catalytic Reduction of 1 While the CV in Figure 2 showed no Faradaic current until the potential became more negative than –2.7 V vs. $Fc^{+/0}$, we saw in Figure

3 that anions of molecules having potentials between –1.9 and –2.7 V can transfer electrons to **1**. Figure 4 confirms that this is true for phenanthrene (**4**). The reversible wave for reduction of of **4** is enhanced by additions of **1**.

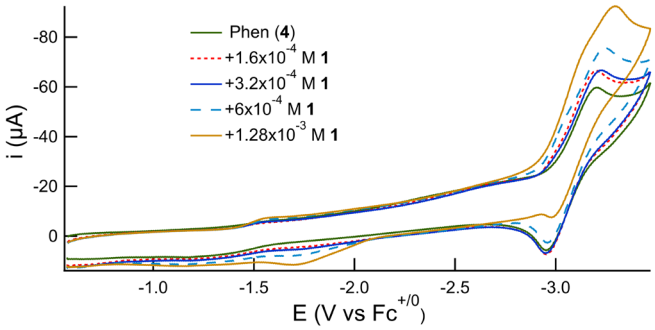

Figure 4. Cyclic voltammograms for reduction of 1 mM 4 alone (black curve) and with subsequent additions of 1×10^{-2} M of **1** in THF with 0.1 M $TBAPF_6$ giving concentrations from 0.2×10^{-4} to 1.28×10^{-3} M of **1**; only the four highest concentrations are shown (1.60×10^{-4} M, 3.20×10^{-4} M, 6.40×10^{-4} M and 1.28×10^{-3} M). The working electrode was glassy carbon.

In THF **4** is reduced at potentials more negative than **1.** Since additions of **1** enhance the sharp peak for reduction of **4**, partial catalytic regeneration of neutral **4** according to the reaction (1) occurs, pointing to the fact, that in the homogeneous phase the reduction of **1** takes place at a less negative potential than heterogeneously at the electrode. A less pronounced, but qualitatively analogous catalytic effect was observed also in reduction of perylene (E^0=-2.12 V vs. $Fc^{+/0}$, Figure S3). These observations further support the conclusion that E^0(**1**) is far more positive than the peak near -3.1 V seen in Figure 2.

Rates from AC Voltammetry and Electrochemical Impedance Spectroscopy

Figure 3 showed that bimolecular ET reactions of **1** slowed by several decades for small driving

force ($-\Delta G^{o}$), so we might expect very slow electrochemical ET near E^{0}, where the driving force is zero. For reduction of **4** the computed reorganization energy is very small, <0.01 eV, so **4** may be expected to provide an example of fast electrochemical reduction. Figure 5 shows the electrochemical rate constant $k(E)$ for **4** reduction evaluated from the AC voltammogram (Figure S8) over a range of DC potentials. The minimum value of $k(E)$, k^{0} = 1.0 cm/s, is observed at –3.01 V vs. $Fc^{+/0}$. This fast rate constant makes analysis of the AC voltammogram possible. Compound **1** yields no Faradaic current at its potential E^{0} given in Figure 3. Instead it is irreversibly reduced at considerably more negative potentials. Very slow ET at such negative potentials is prohibitive for the application of AC polarography. The estimation of the rate constant *k(E)* can be made by electrochemical impedance spectroscopy (EIS). Hence EIS cannot yield the standard heterogeneous rate constant k^{0}.

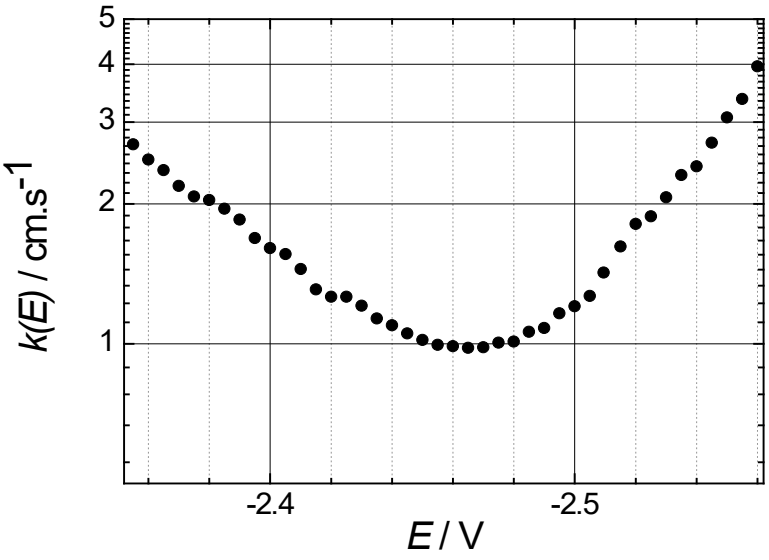

Figure 5. The dependence of the electron transfer rate *k(E)* on the applied DC potential evaluated from the AC voltammogram measured at 16 kHz in acetonitrile (Figure S8).

Figure 6 displays complex impedance plots for **1, 2** and **3**, and Figure 7 displays complex capacitance plots for **1** and **2.**

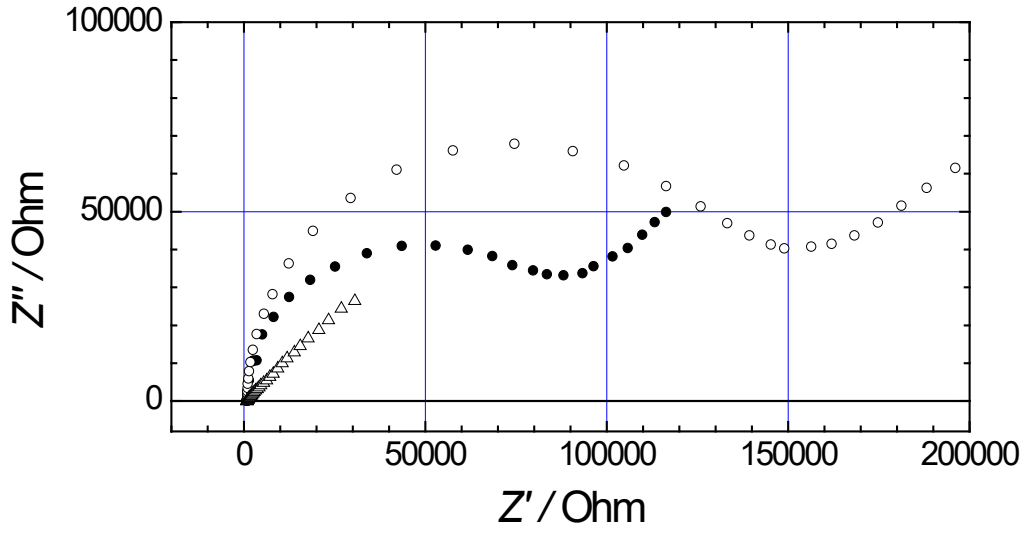

Figure 6. The complex impedance plot of Hg drop electrode in the solution of **1**(○), **2** (●), and **3** (△) in *N*-methyl formamide containing and 0.1 M $TBAPF_6$. The applied DC potentials were the potentials where reduction occurred (–3.15 V (**1**), –3.24 V (**2**) and –2.96 (**3**) vs. $Fc^{+/0}$. The high frequency limit determines the solution resistance 902 Ohm (**1**), 870 Ohm (**2**) and 875 Ohm (**3**).

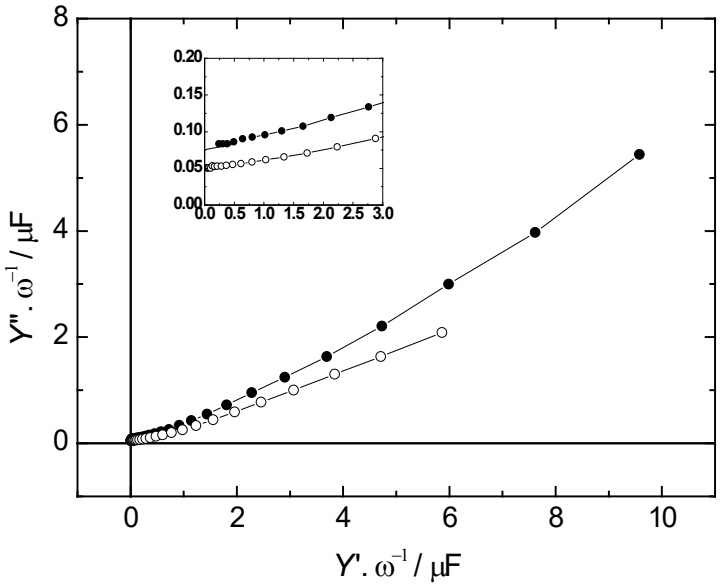

Figure 7. The complex capacitance plot (corrected for the solution resistance) of Hg drop electrode in the solution of **1** (○) and **2** (●) in N-methyl formamide with 0.1 M $TBAPF_6$. The applied DC potentials were those in Figure 6. The inset shows the high frequency limit determining the double layer capacitance 53 nF (**1**) and 87 nF (**2**).

After estimation of the solution resistance (Figure 6) and the double layer capacitance (Figure 7) the dependence of the Faradaic phase angle ϕ on frequency ω is obtained (Figure 8). The heterogeneous electron transfer rate constants for **1** and **2** are calculated from the slope of Figure 8, giving $k(E^0)$ = 0.00194 and 0.00115 respectively. Figure S4 compares this data with that for the planar π molecule **4**, for which we obtained $k(E^0)$ = 1.23 cm/s. EIS spectroscopy thus establishes that at the potentials where reduction was observed, reduction of **1** and **2** occur about 3 orders of magnitude slower than that found for **4**.

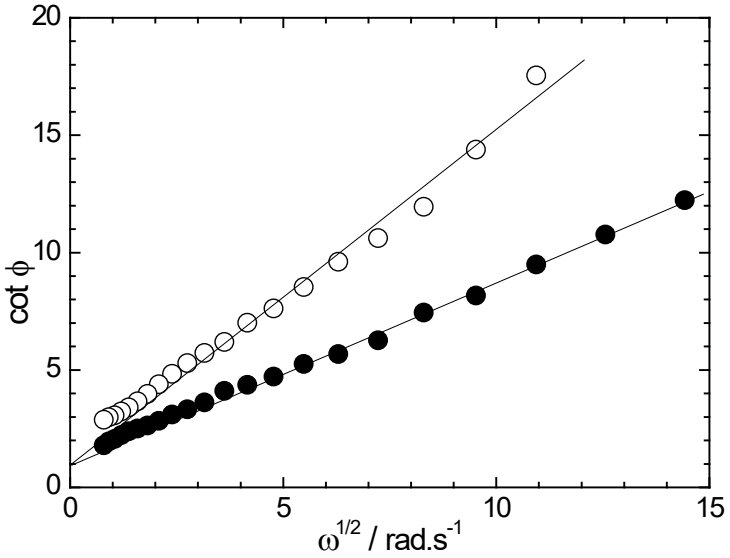

Figure 8. The dependence of the faradaic phase angle ϕ on the applied AC frequency. The slope of the linear dependence yields the electron transfer rate constant $k(E^0)$ = 0.00194 cm s^{-1} for **1** and $k(E^0)$ = 0.00115 cm s^{-1} for **2**. Data were evaluated from Figure 6.

Computed results for ortho-carborane 1. The structural changes in Figure 1 describe massive carbon-carbon bond length changes. Application of the four-point method[28] using b3lyp/d95(d) calculations in THF (PCM) using Gaussian16/Gaussview6[15] yields estimates of reorganization energies of 2.25 eV for converting **1** to $\mathbf{1}^{\bullet-}$ and 1.25 eV for converting $\mathbf{1}^{\bullet-}$ to **1**. These large reorganization energies would be expected to greatly slow weakly-exoergic electron transfer. In Figure 2, Ac_2Bz gave a slow bimolecular ET rate with **1**, and resulted in an equilibrium giving ΔG^o = 0.032 eV, so we might expect these two molecules to share an electron almost equally. Figure 9 shows relaxed potential energy surface scans (b3lyp/6-31g(d)/THF) in which the C-C distance in **1** was varied while all other coordinates were optimized at each value of the C-C distance.

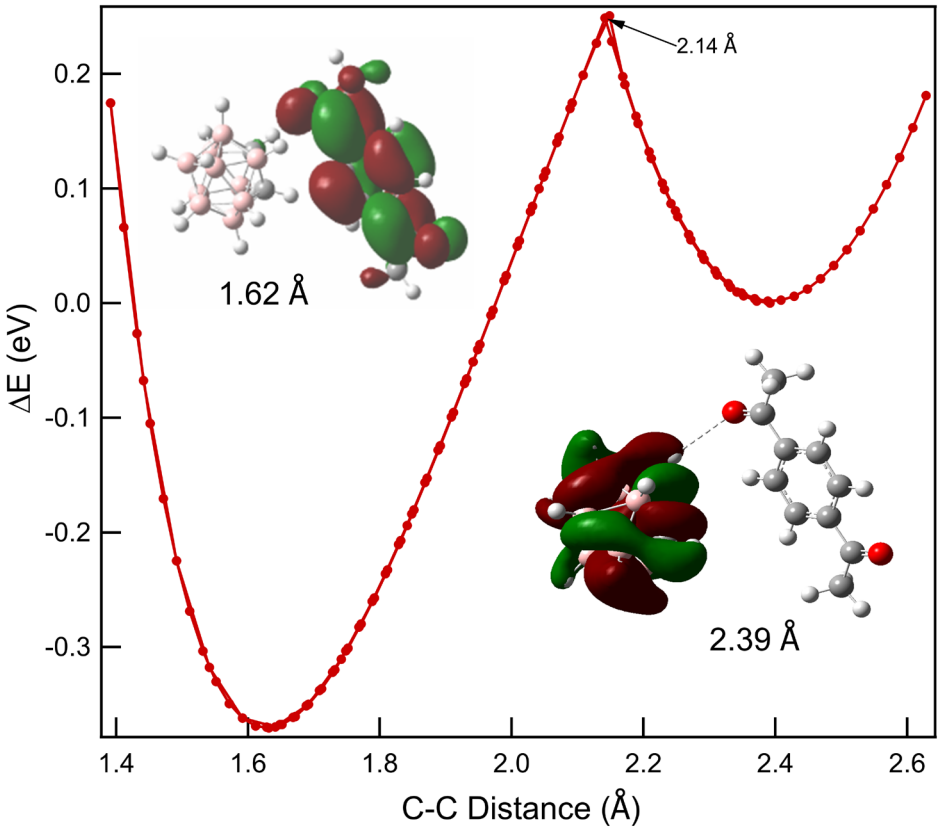

Figure 9. B3lyp/6-31g(d) (SCRF,THF) scans of a the energy of complex (Ac_2Bz,**1**) with one added electron. At the left hand minimum, where the C–C distance R_{cc} = 1.62 Å and for all points with R_{CC} < 2.14 Å the excess electron is on Ac_2Bz (left inset) and for R_{CC} > 2.14 Å the electron is on **1** (right inset).

In Figure 9 the difference between the two minima is 0.371 eV, which is very different from ΔG^o (Ac2Bz$^{\bullet-}$ + **1**) = 32 ± 10 meV measured from bimolecular ET reactions in Figure 2, but the 0.371 eV is an enthalpy difference between the 2 complexes, and not free ions. The reactant and product curves in Figure 9 cross at a point 0.62 eV above the reactant minimum and 0.25 eV above the product minimum. If the reaction really has ΔG^o ~0 then its activation energy might be

near the average, 0.435 eV. The Boltzmann factor for surmounting this barrier is 4×10^{-8} supporting the idea of very slow ET rates, although this estimate may contain substantial error because it is an energy, not a free energy.

While the scans in Figure 9 are enthalpies, frequency calculations employed at selected points to provide better estimates. These free energy estimates, also using b3lyp/6-31g(d)/THF, predict ΔG^o= –0.057 eV for electron transfer from free $Ac_2Bz^{\bullet-}$ to **1** in reasonable agreement with the experimental result ΔG^o = 0.032 eV presented with Figure 2. Free energies further differ by only 0.166 eV for the optimized complexes in Figure 9, suggesting that the actual PES curves would cross at closer to the average C-C bond distance of the 2 complexes. One can approximately shift the enthalpy curves above to the calculated ΔG^o = 0.166 eV between the complexes. This yields a rough estimate of a 0.33 eV for the barrier, giving a smaller Boltzmann factor, 2×10^{-6}, still predicting 6 order of magnitude impediment to the ET rate

Table 1 presents computed energetics for reduction and oxidation of **1**. Optimization of $\mathbf{1}^{\bullet-}$ found the highly distorted state $\mathbf{1}^{\bullet-}_{Ad2}$ only if the initial structure was distorted from that of neutral **1** by lengthening the C-C bond. In addition, some intermediate structures were identified. For each structure Table 1 reports the energy relative to that of the optimized neutral, E(A) – E(N), and the reduction potential, E_r, estimated by eq 5,

$$E_r = -(E(A^{\bullet-}) - E(N)) + (E(Ac_2Bz^{\bullet-}) - E(Ac_2Bz)) - 1.890 \qquad (6)$$

where –1.890 V is the known reduction potential of Ac_2Bz.[22] Potentials estimated by eq 6 for varied conformations of $\mathbf{1}^{\bullet-}$ will be considered in the discussion as candidates for the species formed in the observed reduction waves in figure 2a).

Table 1 Computed Energetics for Reduction and Oxidation of **1** estimated by b3lyp/d95(d)// b3lypy/6-31g(d) using the PCM model for THF.

Species [a]	E(A) – E(N) eV [b]	E_r (V vs. $Fc^{+/0}$) [c]
$\mathbf{1}/\mathbf{1}^{\bullet-}_{v}$	–0.26	-4.21
$\mathbf{1}/\mathbf{1}^{\bullet-}_{As}$	–0.69	-3.78
$\mathbf{1}/\mathbf{1}^{\bullet-}_{Ad1}$	–1.42	–3.05
$\mathbf{1}/\mathbf{1}^{\bullet-}_{Ad2}$	–2.51	–1.96
$\mathbf{1}^{\bullet-}_{Ad2}/\mathbf{1}^{-2}$	–2.15 [d]	-2.32
$\mathbf{1}^{\bullet+}/\mathbf{1}$	8.362	3.89
$Ac_2Bz/Ac_2Bz^{\bullet-}$	–2.59	–1.89

[a] Geometries of **1**: v=vertical anion (at geometry of neutral); As=optimized with or without symmetry enforced, starting with the symmetric (C_{2v}) neutral geometry; A_{d1}=optimized without symmetry after a manual distortion, giving a local minimum; A_{d2}=optimized starting from a structure with a lengthened C-C bond, giving the lowest energy radical anion. All geometries except A_s gave no imaginary frequencies.

[b] Energy of the anion or cation, E(A) - energy of the neutral, E(N).

[c] Reduction potential vs. $Fc^{+/0}$ calculated from the energy differences in column 2 and the measured reduction potential –1.890 V vs. $Fc^{+/0}$ for Ac_2Bz.[22]

[d] $E(\mathbf{1}^{-2}) – E(\mathbf{1}^{\bullet-}_{Ad2})$

Discussion

The experimental data above display sometimes astonishing effects of the large structural changes upon electron attachment to **1**. This discussion section will seek to understand these with emphasis on two observations:

1. The reduction potential determined from equilibria is E^0 ($\mathbf{1}^{0/-}$) = –1.92 V vs. $Fc^{+/0}$**,** but a wave for its reduction by polarography and cyclic voltammetry appears at ~ –3.15 V vs. $Fc^{+/0}$, more negative by more than 1.2 V.
2. The electrochemical rate constant k_s(**1**) at E^0 ($\mathbf{1}^{0/-}$) = –1.92 V vs. $Fc^{+/0}$ is certainly small given that no Faradaic current appears at the potential. But what is k_s(**1**) at E^0 ($\mathbf{1}^{0/-}$) and how does reduction actually proceed at much more negative potentials?

The Reduction Potential of 1 was determined in three ways. The first, noted above, is by equilibrium with Ac_2Bz to be E^0 ($\mathbf{1}^{0/-}$) = –1.92 ± 0.01 V vs. $Fc^{+/0}$. The second utilizes fits to rate vs ΔG^o for 20 compounds in Figure 3. The measured bimolecular rate constants in Figure 3 for electron transfer ET to **1** and from $\mathbf{1}^{\bullet-}$ were fit as a function of free energy change using a common expression with an electronic coupling, H_{ab}, a solvent reorganization energy, λ_s=0.5 eV, an internal reorganization energy, λ_v= 1.66 eV, for a vibrational mode with a frequency of 1400 cm^{-1}. The fits also included a diffusion-controlled limit of 9.9×10^9 $M^{-1}s^{-1}$. Adjusting E^0(**1**) during the fit to give origins to the scales for both ET to **1** and from $\mathbf{1}^{\bullet-}$ converged to yield E^0 ($\mathbf{1}^{0/-}$) = –1.9 ± 0.030 V vs. $Fc^{+/0}$ in good agreement with the potential from the equilibrium with Ac_2Bz. The two fit curves crossed at k_{Bi} = 2×10^5 $M^{-1}s^{-1}$. Thirdly computations estimated E^0. Optimization (b3lyp/6-31g*) of **1** and $\mathbf{1}^{\bullet-}$ in the PCM reaction field for THF found $\mathbf{1}^{\bullet-}$ to be 2.51 eV more stable than **1**, corresponding to a reduction potential of –1.96 V vs. $Fc^{+/0}$ in agreement with potentials determined by electron transfer.

At odds with these three determinations is observations of waves with peaks/waves in the DC-polarography or CV's of Figure 2a) and S2 at –3.1 to –3.3 V vs. $Fc^{+/0}$, depending the solvent, suggesting that E^0($\mathbf{1}^{0/-}$) is near –3.2 V vs. $Fc^{+/0}$. Those observations are countermanded by the

mediated ("catalytic") reductions in Figure 4 which suggests that $E^0(\mathbf{1}^{0/-})$ is more positive than –2.12 vs. $Fc^{+/0}$. We conclude that $E^0(\mathbf{1}^{0/-})$ is very close to –1.9 V vs. $Fc^{+/0}$ but that ET reactions operating at this potential may be very slow. How slow is not clear.

As seen earlier for reduction of a dicarborane (**2**),[29] optimization of $\mathbf{1}^{\bullet-}$ starting at the structure of **1** did not proceed to the lowest energy structure for $\mathbf{1}^{\bullet-}$ without intervention,[29] suggesting that addition of an electron to of **1** would not easily lead to the most stable conformer of $\mathbf{1}^{\bullet-}$. Formation of $\mathbf{1}^{\bullet-}$ at an electrode or through bimolecular reactions might conceivably occur by electron attachment to form the symmetric $\mathbf{1}^{\bullet-}_{As}$ or partly distorted $\mathbf{1}^{\bullet-}_{Ad1}$ state listed in Table 1, followed by relaxation to the highly distorted $\mathbf{1}^{\bullet-}_{Ad2}$. Potential scans in Figure S10 indicate possible routes.

The Fate of Reduced 1. CV's in Figure 2 show oxidation peaks on reverse scans, but none appear to be reoxidation of $\mathbf{1}^{\bullet-}$. We have interpreted the reduction as producing the highly distorted $\mathbf{1}^{\bullet-}$, plausibly $\mathbf{1}^{\bullet-}_{Ad2}$ in Table 1. The computations also found that this species would be very resistant to protonation. From computed estimates of energetics in Table 1 we can see that in sweeping to –3.3 V vs. $Fc^{+/0}$ we should not be able to form the "vertical" anion, $\mathbf{1}^{\bullet-}_{v}$ at the geometry of the neutral or the symmetric anion, $\mathbf{1}^{\bullet-}_{As}$, but it should be possible to form the distorted $\mathbf{1}^{\bullet-}_{Ad1}$, though 4 point reorganization energies find similarly substantial reorganization energy to form $\mathbf{1}^{\bullet-}_{Ad1}$ as $\mathbf{1}^{\bullet-}_{Ad2,}$ suggesting slow rates. The computed energetics also indicate that $\mathbf{1}^{\bullet-}_{Ad2}$ may accept a second electron. The estimated redox potential, -2.32 V in Table 1, is 0.36 V more negative than the single-electron reduction to form $\mathbf{1}^{\bullet-}_{Ad2,}$ but this computed estimate does not include the effect of the $TBAPF_6$ electrolyte. Strong ion pairing with $\mathbf{1}^{-2}$ with TBA^+ could stabilize the dianion sufficiently that it is formed more easily. Either this or the previous possibility could explain the observation of 1.7 electron consumed in the reduction. Once $\mathbf{1}^{2-}$ is

produced it is very readily protonated, for example by a neutral **1** molecule, so it is likely that **1** is doubly reduced and then protonated. Double reduction followed by protonation can thus explain the irreversibility observed by CV, and the products of protonation are plausible candidates for the observed oxidation waves in figure 2. Alternatively protonation might occur after one electron reduction. This possibility can not be dismissed although computational energetics militate against it.

We note that in the pulse radiolysis experiments **1** is reduced either by solvated electrons or one of the several $D^{\bullet-}$ anions. In either case only one electron is available, so $\mathbf{1}^{\bullet-}$ can be produced, but not $\mathbf{1}^{2-}$.

Electron Transfer Rate Constants Electron transfer at electrodes and bimolecular electron transfer between molecules in solution can be compared using the theory of Marcus,[1] which described both in terms of an activation free energy, ΔG^*. For the planar hydrocarbon, **4** (**3**) ac voltammetry found $k(E^0) = 1.0$ cm/s (Figure 5) and impedance spectroscopy results described above yielded a heterogeneous electrochemical rate constant of $k(E^0,\mathbf{4}) = 1.23$ cm/s at the formal potential where the free energy change ΔG^o equals zero. The rate constant k_s was ~1000 times slower for **1**, but this was at –3.15 V vs. $Fc^{+/0}$, which is 1.23 V more negative than E^0. We may guess that $k^0(E^0)$ is smaller, perhaps by many decades, a result supported by DigiSim simulations, but the measurements by impedance spectroscopy could not actually determine $k(E^0,\mathbf{1})$.

Fits to bimolecular ET rate constants in Figure 3 crossed at $k_{Bi} = 2\times10^5$ $M^{-1}s^{-1}$, nearly 5 decades slower than the faster rate constants. The approach to equilibrium between $\mathbf{1}^{\bullet-}$ and Ac_2Bz occurred with $k_{Bi} = 1\times10^6$ $M^{-1}s^{-1}$ so k_{Bi} changed by 4-4.7 decades. For use in discussion below we average this to 4.4 decades. Computed free energies for ET in a complex of **1** and

Ac_2Bz gave a barrier for ET and a roughly 6 decade inhibition in rate from what might have been possible in a contact pair of molecules.

An estimate for $k(E^0)$ for **1** comes from the DigiSim (Marcus-Hush) simulation using a reorganization energy of 2.16 eV, consistent with results in Figure 3 for reactions of **1**. The simulation used $E^0(\mathbf{1}^{0/-}) = -1.92$ V and $k_s = 6\times10^{-12}$ cm/s which produced a peak at –3.1 V in THF. This k_s is 11.2 decades smaller than that for the planar molecule **4**, in stark contrast to the rate constants in Figure 3, for which we see a 4.4 decade (average) decrease, not 11.2. Below we examine some of the assumptions underlying this 6+ decade discrepancy. We will find that we can remove a few decades from the ~6.8 decade discrepancy.

We first note that the redox potential of Ac_2Bz was determined in DMF as were those of most the D and A molecules used in Figure 3, so while Figure 3 studies reactions in THF, our estimate of the redox potential of **1** should use potentials in DMF. In DMF the CV of **1** peaks at a more positive potential and is better described by a simulation with $k_s = 1.5\times10^{-11}$ cm s^{-1}, removing 0.4 decade from the discrepancy.

A larger contribution may come from the diffusion-control limit near 1×10^{10} $M^{-1}s^{-1}$ on bimolecular rate constants of **1** in Figure 3. The electrochemical rate constant is plausibly near 10^{-11} cm s^{-1} at $E^0(\mathbf{1}^{0/-}) = -1.92$ V and rises by several decades to $k_s = 0.00194$ cm/s at –3.1 V. By comparison, the bimolecular reactions have rate constants near $0.2\text{-}1\times10^6$ $M^{-1}s^{-1}$ at –1.92 V but rise only to the diffusion-control limit at 1×10^{10} $M^{-1}s^{-1}$ over the same 1.2 V range. But estimates from distance-dependent reaction in glasses found that the electronic coupling between two molecules in contact is sufficiently strong to give ET with rates 400 times faster than the diffusion-control limit. A corollary is that without the diffusion-control limit the rates in Figure 3

would have varied over a range 2.6 decade smaller range, or 4.4 decades, reducing the discrepancy between the rise of electrochemical and bimolecular rates.

With the rough corrections just described the discrepancy between electrochemical and bimolecular ET rate constants is reduced. While additional factors may further reduce it or add to it, the discrepancy, ~4.4 decades, remains large. Marcus' 1965 paper unified theory for ET in homogeneous solution and at electrodes, concluding the for the same molecules changes in rates should be similar, apart from a square for self-exchange reactions for which the reorganization energy is the sum of λ from the two identical molecules. For the bimolecular ET reactions of **1** with conjugated molecules the reorganization energy, λ_v, is dominated by the contribution from **1**, so neglect of the contribution from the conjugated molecules is an error, but a modest one. So should we expect that the same driving force, an applied voltage in the electrochemical case and a redox potential difference in bimolecular ET, would produce the same range of rate constants? In Figure 10 we argue that the answer is no, but only because the driving force is different.

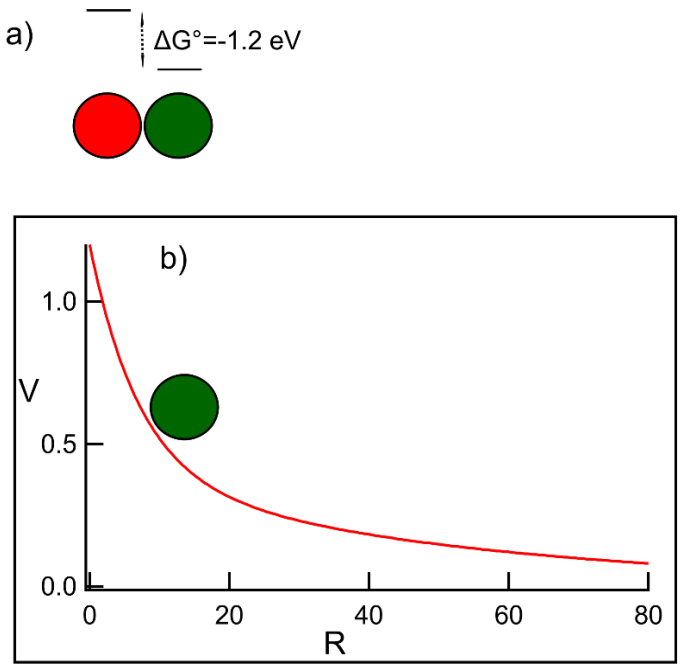

Figure 10 a) Donor and acceptor molecules next to each other having a difference of redox potentials $\Delta G^{\circ} = E^{0}(\mathrm{A}) - E^{0}(\mathrm{D})$. b) A molecule approaching an electrode. The double-layer potential is pictured schematically (red line).

In Figure 10 a) the entire $\Delta G^{\circ} = E^{0}(\mathrm{A}) - E^{0}(\mathrm{D})$ is available to drive electron transfer, but in 10 b) because the double-layer falls somewhat gradually with distance,[18,30] only part of the total potential drop is available to drive electron transfer, and the potential available depends on how close the molecule gets to the electrode. This role of the double-layer is one aspect of the Frumkin effects.[31,32] The large reorganization energy for electron transfer to or from **1** causes large decreases in ET rates at $\Delta G^{\circ} = 0$. If we assume that the reorganization causes bimolecular ET rates fall by a factor of 10^6 ($\sim 10^4$ observed and 10^2 hidden by diffusion control) and that the electrochemical rate constant should fall by the same factor, then we may reinterpret the DigiSim simulations in Figure 2a) to indicate that the 1.2 V difference between the observed CV wave and $E^{0}(\mathbf{1}^{0/-}) = -1.92$ V is comprised of a 0.72 V actual driving force and 0.48 V that was the unavailable part of the voltage in the double-layer.

Comparison of Earlier Work The interpretation mentioned above described reduction of **1** in solution and at electrodes as a single-step ET process with a very large reorganization energy. It is valuable to compare with the results of Evans and coworkers[5-7] who observed that large structure changes produced distinct steps best understood in terms of a "square" kinetic scheme. In common with their results the present work found that two electrons are involved in electrochemical reduction, although only one electron is possible in the bimolecular ET in Figure 3. Both the Evans results and the present work report CV's for reductions that show no reverse waves near the reduction waves. Differences are that the electrochemical rate constants in the

Evans work are typically 0.01-0.25 cm/s [6] while they are probably about ten decades smaller for **1**. The Evans results indicated that the actual reductions were reversible, and produced waves at or close to E^0, but were followed by structural relaxations. While Evans did not study bimolecular ET, the large, 10^4-10^5 reduction of rate constants observed for **1** in Figure 3 as $\Delta G°$ approaches zero would not be expected for the Evans' molecules. In support the computed surfaces in Figure S10 indicate the ET should be very slow if $\Delta G°$ approaches zero. We conclude that the present results bear resemblances to those of Evans[5-7] but in **1** the ET occurs with large structure changes which are necessary for ET to occur, while in their molecules structure changes occurred after ET.

Conclusions

The reduction potential of **1** is –1.92 V vs. $Fc^{+/0}$ based on bimolecular equilibria, fits to 20 ET rate constants in solution, computation and electrochemical catalysis. But due to the large structural change in $\mathbf{1}^{\bullet-}$ electrochemical measurements (DC-polarograms as well as cyclic voltammograms) show no reduction until –3.1 V vs. $Fc^{+/0}$, ~1.2 V negative of E^0. The large shift of the CV due to the massive reorganization energy on converting **1** to $\mathbf{1}^{\bullet-}$ causes electron transfer rates to be too small to produce observable current until the overpotential is ~1.2 V. A comparison to changes of bimolecular ET rates with k_{Bi} leads to the estimate that about 40% of this overpotential arises because the double layer structure does not make all of the applied voltage available to drive electron transfer, a manifestation of the Frumkin effects. The present results are best described in terms of ET with large reorganization energy, in contrast to the separate ET and reorganization steps well described[5-7] by a "square" kinetic scheme.

ASSOCIATED CONTENT

Supporting Information. Additional voltammograms, examples of transient absorption to obtain rate constants, a graph of Faradaic phase angles used in evaluating electrochemical rate constants and a graph of computed potential energy surfaces for the title compound. The following files are available free of charge.

brief description (file type, i.e., PDF)

brief description (file type, i.e., PDF)

AUTHOR INFORMATION

Corresponding Author

John R. Miller, jrmiller@bnl.gov

ORCID

Andrew R. Cook: 0000-0001-6633-3447

John R. Miller: 0000-0003-4377-7445

Author Contributions

The manuscript was written through contributions of all authors. All authors have given approval to the final version of the manuscript.

ACKNOWLEDGMENT

This material is based upon work by JRM and AC supported by the U.S. Department of Energy, Office of Science, Office of Basic Energy Sciences through Grant DE-SC00112704**,** including use of the LEAF and Van de Graaff facilities of the BNL Accelerator Center for Energy Research. Work in the Prague laboratorieswas supported by the Czech Academy of Sciences

(RVO: 61388963, 61388955). JM thanks the Czech Academy of Sciences (RVO: 61388963) and to GAČR grant 19-22806S and NSF, grant CHE 1566435. We are grateful to Dr. Yves-Marie Hervault for synthesis of the Me_8-o-carborane.

ABBREVIATIONS

.

REFERENCES

1. Marcus, R. A. "On the Theory of Electron-Transfer Reactions. Vi. Unified Treatment for Homogeneous and Electrode Reactions.", *J. Chem. Phys.,* **1965**, *43*, 679-701.
2. Marcus, R. A. "On the Theory of Oxidation-Reduction Reactions Involving Electron Transfer .1", *J. Chem. Phys.,* **1956**, *24*, 966-978.
3. Parson, W. W.; Chu, Z. T.; Warshel, A. "Reorganization Energy of the Initial Electron-Transfer Step in Photosynthetic Bacterial Reaction Centers", *Biophys. J.,* **1998**, *74*, 182-191.
4. Zhang, X. X.; Bowen, K. "A Photoelectron Spectroscopic and Computational Study of the O-Dicarbadodecaborane Parent Anion", *J. Chem. Phys.,* **2016**, *144*.
5. Hu, K.; Evans, D. H. "Electron-Transfer Reactions with Significant Inner Reorganization Energies. Two-Electron Oxidation of Derivatives of 1,4-Bis(Dialkylamino)-1,3-Butadiene", *J. Phys. Chem.,* **1996**, *100*, 3030-3036.
6. Macías-Ruvalcaba, N. A.; Evans, D. H. "Electron-Transfer Reactions with Significant Changes in Structure. Unsymmetrical Crowded Ethylenes", *J. Phys. Chem. B,* **2006**, *110*, 24786-24795.
7. Lachmanová, Š.; Dupeyre, G.; Tarábek, J.; Ochsenbein, P.; Perruchot, C.; Ciofini, I.; Hromadová, M.; Pospíšil, L.; Lainé, P. P. "Kinetics of Multielectron Transfers and Redox-Induced Structural Changes in N-Aryl-Expanded Pyridiniums: Establishing Their Unusual, Versatile Electrophoric Activity", *J. Am. Chem. Soc.,* **2015**, *137*, 11349-11364.
8. Nelsen, S. F.; Ismagilov, R. F.; Gentile, K. E.; Nagy, M. A.; Tran, H. Q.; Qu, Q. L.; Halfen, D. T.; Odegard, A. L.; Pladziewicz, J. R. "Indirect Determination of Self-Exchange Electron Transfer Rate Constants", *J. Am. Chem. Soc.,* **1998**, *120*, 8230-8240.
9. Rillema, D. P.; Endicott, J. F.; Kanemagu.Na "Self-Exchange Reactions of Cobalt Complexes and Implications Concerning Redox Reactivity of Vitamin-B12", *J. Chem. Soc., Chem. Commun.,* **1972**, 495-6.

10. Nelsen, S. F.; Kinlen, P. J.; Evans, D. H. "Comparison of Proton-Transfer and Electron-Transfer Equilibria and Rates for Tetraalkylhydrazines", *J. Am. Chem. Soc.,* **1981**, *103*, 7045-7050.
11. Endicott, J. F.; Durham, B.; Kumar, K. "Examination of the Intrinsic Barrier to Electron Transfer in Hexaaquacobalt(Iii): Evidence for Very Slow Outer-Sphere Self-Exchange Resulting from Contributions of Franck-Condon and Electronic Terms", *Inorg. Chem.,* **1982**, *21*, 2437-2444.
12. Ullman, A. M.; Nocera, D. G. "Mechanism of Cobalt Self-Exchange Electron Transfer", *J. Am. Chem. Soc.,* **2013**, *135*, 15053-15061.
13. Herzog, A.; Maderna, A.; Harakas, G. N.; Knobler, C. B.; Hawthorne, M. F. "A Camouflaged Nido-Carborane Anion: Facile Synthesis of Octa-B-Methyl-1,2-Dicarba-Closo-Dodecaborane(12) and Its Deboration Reaction", *Chem. Eur. J.,* **1999**, *5*, 1212-1217.
14. Wishart, J. F.; Cook, A. R.; Miller, J. R. "The Leaf Picosecond Pulse Radiolysis Facility at Brookhaven National Laboratory", *Rev. Sci. Inst.,* **2004**, *75*, 4359-4366.
15. Frisch, M. J.*et al.*,"Gaussian 16", 2016, Wallingford CT.
16. Rudolph, M.; Feldberg, S. W.,"Digisim 3.03b", 2004, West Lafayette, IA.
17. Hong, S. H.; Evans, D. H.; Nelsen, S. F.; Ismagilov, R. F. "Evidence for a Two-Step Electron-Transfer Process in the Electrode Reactions of Tetraisopropylhydrazine, Tetracyclohexylhydrazine and Their Radical Cation Salts", *J. Electroanal. Chem.,* **2000**, *486*, 75-84.
18. Bard, A. J.; Faulkner, L. R. *Electrochemical Methods: Fundamentals and Applications*; John Wiley & Sons, 2001.
19. Chidsey, C. E. D. "Free Energy and Temperature Dependence of Electron Transfer at the Metal Electrolyte Interface", *Science,* **1991**, *251*, 919.
20. Zakharkin, L. I.; Kalinin, V. N. "The Transfer of Electrons in the Carborane Series", *Bulletin of the Academy of Sciences of the USSR, Division of chemical science,* **1970**, *19*, 2246-2248.
21. Gingrich, H. L.; Ghosh, T.; Huang, Q.; Jones, M. "1,2-Dehydro-Ortho-Carborane", *J. Am. Chem. Soc.,* **1990**, *112*, 4082-4083.
22. Pedersen, S. U.; Christensen, T. B.; Thomasen, T.; Daasbjerg, K. "New Methods for the Accurate Determination of Extinction and Diffusion Coefficients of Aromatic and Heteroaromatic Radical Anions in N,N-Dimethylformamide", *J. Electroanal. Chem.,* **1998**, *454*, 123-143.
23. Levich, V. G. In *Adv. Electrochem. Electrochem .Eng.*; Delahay, Tobias, Eds.; Wiley: New York, 1966; Vol. 4, p 249.
24. Fischer, S. F.; Van Duyne, R. P. "On the Theory of Electron Transfer Reactions. The Naphthalene-/Tcnq System", *Chem. Phys.,* **1977**, *26*, 9-16.
25. Miller, J. R.; Beitz, J. V.; Huddleston, R. K. "Effect of Free Energy on Rates of Electron Transfer between Molecules", *J. Am. Chem. Soc.,* **1984**, *106*, 5057-68.
26. Marcus, R. A.; Siders, P. "Theory of Highly Exothermic Electron-Transfer Reactions", *J. Phys. Chem.,* **1982**, *86*, 622-630.
27. Waite, T. R. "Theoretical Treatment of the Kinetics of Diffusion-Limited Reactions", *Physical Review,* **1957**, *107*, 463-470.
28. Nelsen, S. F.; Blackstock, S. C.; Kim, Y. "Estimation of Inner Shell Marcus Terms for Amino Nitrogen Compounds by Molecular Orbital Calculations", *J. Am. Chem. Soc.,* **1987**, *109*, 677-682.

29. Cook, A. R.; Valášek, M.; Funston, A. M.; Poliakov, P.; Michl, J.; Miller, J. R. "P-Carborane Conjugation in Radical Anions of Cage–Cage and Cage–Phenyl Compounds", *J. Phys. Chem. A,* **2018**, *122*, 798-810.
30. Stojek, Z. In *Electroanalytical Methods*; 1 ed.; Scholz, F., Ed.; Springer-Verlag 2005: Berlin Heidelberg, 2005, p 331.
31. Frumkin, A. "Hydrogen Overvoltage and the Structure of the Double Layer", *Zeitschrift Fur Physikalische Chemie-Abteilung a-Chemische Thermodynamik Kinetik Elektrochemie Eigenschaftslehre,* **1933**, *164*, 121-133.
32. Oldham, K.; Myland, J. *Electrochemical Science and Technology: Fundamentals and Applications*; John Wiley and Sons: Chichester, United Kingdom, 2012.